INTERNATIONAL JOURNAL FOR NUMERICAL METHODS IN FLUIDS
Int. J. Numer. Meth. Fluids 2008; **57**:583–600
Published online 19 March 2008 in Wiley InterScience (www.interscience.wiley.com). DOI: 10.1002/fld.1764

A two-dimensional prototype multi-physics model of the right ventricle of the heart

T. N. Croft*,†, A. J. Williams, A. K. Slone and M. Cross

Centre for Civil and Computational Engineering, School of Engineering, University of Wales Swansea, Swansea, U.K.

SUMMARY

The heart operates as a delicate function of the interactions among its electro-chemical, structural and fluid components. The objective of this paper is to describe the computational modelling of the interaction between simplified forms of the electro-chemical, structural and fluid behaviour. It is because the objective here is to evaluate the interactions among the phenomena that the specific models of the electro-chemical, fluid and structural behaviour are kept as simple as possible. The electro-chemical model is drawn from that of Clayton and Holden, while the blood is assumed to be a conventional slightly compressible Navier–Stokes fluid and the heart wall is a simple elastic structure modelled via the static equations. The model is implemented within a multi-physics finite volume solver environment using an unstructured mesh approach, which enables the implementation of models for each of the specific phenomenon and their interactions. The model is two dimensional, but shows how the electric field drives a cross section of the wall so that it pumps the blood in and out of the right ventricle geometry. Copyright © 2008 John Wiley & Sons, Ltd.

Received 13 July 2007; Revised 12 October 2007; Accepted 3 December 2007

KEY WORDS: fluid–structure interaction; electro-chemical models; mesh movement; multi-physics; finite volume methods

1. INTRODUCTION

The function of the human heart is extremely complex and unravelling its mysteries has engaged clinical scientists for generations. During the last decade, notably inspired by Noble [1], considerable progress has been made in understanding the electro-chemical behaviour of the heart. This knowledge has been embedded within increasingly sophisticated mathematical models. Starting from the Hodgkin–Huxley paradigm model [2] for squid nerve action potential, Noble [3] adapted it in 1960 as a means to investigate cardiac action, and spawned an enduring worldwide iterative modelling and experimental activity to develop a very sophisticated understanding of the electro-chemical

*Correspondence to: T. N. Croft, Centre for Civil and Computational Engineering, School of Engineering, University of Wales Swansea, Swansea, U.K.
†E-mail: t.n.croft@swansea.ac.uk

behaviour of the heart. This understanding has been embedded within a wide range of mathematical models, normally based on what are called bi-domain equations, of which those by the teams of Trayanova *et al.* [4], Plank and Vigmond [5], Sundnes [6] are typical, although probably the most comprehensive is due to the work of Noble and co-workers [7]. This work has provided the basis for genuine significantly functional virtual heart models that may be used in clinical research and treatment assessment. These models would be enhanced if they could be embedded within suitable models of the fluid–structure interaction between the blood and heart wall.

Considerable work on the mechanics of the heart has been led over the years by Nickerson and co-workers [8] such as Smith *et al*. [9], Nash and Hunter [10] and LeGrice *et al*. [11]. Based on the work of Costa *et al*. [12] the structure of the heart wall has been characterized and recorded digitally. Hunter and his team, together with others, notably Markhasin *et al.* [13] and Nash and Panifilov [14], have developed a range of models to capture the behaviour of the heart wall, with respect to both its detailed geometric structure and its non-linear material properties. There have been a number of attempts to capture the interaction between an electro-chemical bi-domain model and a structural response, where notable contributions are by Smith [15], Haslach [16], Usyk *et al*. [17] and Arts *et al*. [18].

Another aspect of the heart modelling challenge that has engaged attention has been that of the fluid–structure interaction to capture the pumping action of the heart. This is a significant challenge simply because the capture of transient fluid–structure interaction processes is itself regarded as extremely challenging from a computational perspective, for example, see Farhat *et al.* [19], Mok and Wall [20], Mattheis and Steindorf [21] and Slone *et al*. [22, 23]. There are a variety of reasons for this challenge including the conventionally disparate discretization approaches used for solving for fluid and structural dynamics, the numerical difficulties of enabling stable application of boundary conditions between the fluid and structure, and accounting for the impact of dynamic changes in the domain geometry, to name but three! The most significant progress in the context of the heart has been made by Peskin and McQueen [24, 25], McQueen and Peskin [26] and Kovacs *et al*. [27] who have used what is termed the immersed boundary method whereby each element in the mesh is defined as a fluid or solid depending on its local conditions. More recently, there have been other attempts at modelling an aorta or a ventricle by de Hart *et al.* [28], Patterson *et al*. [29], and Carmody *et al*. [30] among others. These models capture the interaction between the 'blood' and the heart wall, but still require the wall dynamic deformation to be specified (in reality, of course, this is a consequence of the electro-chemical action).

The only work to address the complete electro-chemical-fluid–structure interaction is by Watanabe *et al*. [31] who developed a two-dimensional model based on an electro-chemical model of Luo and Rudy [32] although the structural movement was somewhat restricted. In this contribution, we describe a two-dimensional model that captures the impact of a cyclic electric field (arising from Clayton and Holden's electro-chemical model [33]) on a right ventricle geometric structure containing a 'blood'-like fluid, simulating both its filling and emptying.

2. THE COMPUTATIONAL MODEL

2.1. Overview of the mathematical model

As indicated above the computational model is concerned with an idealized geometry of a right ventricle of a human heart, illustrated in Figure 1, with dimensions extracted from a variety of

DOI: 10.1002/fld

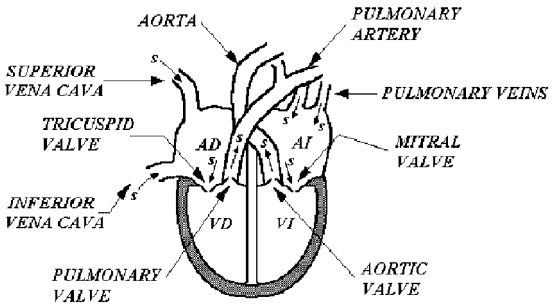

Figure 1. An illustration of the cross section of a human heart showing the key fluid and structural functions, taken from www.heartvalves.8m.com.

sources including [34]. The model itself has three components:

(a) a cyclic electro-chemical model;
(b) a fluid model to describe the flow of 'blood';
(c) a structural model to describe the contraction and relaxation of the 'heart' wall in response to the cyclic electric field;

and their interactions.

2.1.1. Clayton and Holden's electro-chemical model. The Clayton–Holden model [33] is essentially an attempt to capture the action potential propagation throughout the ventricle as a continuous mono-domain. It is based largely on the work of Fenton and Karma [35] who proposed a membrane voltage, V_m, given by a cable equation and including a membrane patch current, I_{ion}, which include equations to capture the fast and slow inward (depolarizing) currents corresponding broadly to Na^+ and Ca^{2+} currents and a slow outward (polarizing) current corresponding to K^+ currents.

The membrane voltage, V_m, is scaled with both the resting potential, V_0, and the Nernst potential of the fast inward current, V_{fi}, as follows:

$$u = (V_m - V_0)/(V_{fi} - V_0) \tag{1}$$

Using this approach, the Clayton–Holden model may then be summarized as the combination of a primary, u, and two secondary, v and w, action potentials:

$$\begin{aligned}
\frac{\partial u}{\partial t} &= \nabla \cdot \mathbf{D} \nabla u - (J_{fi} + J_{si} + J_{so}) \\
\frac{\partial v}{\partial t} &= \Theta(u_c - u)\left[\frac{1-v}{t_v^-(u)}\right] - \Theta(u - u_c)\left[\frac{v}{t_v^+}\right] \\
\frac{\partial w}{\partial t} &= \Theta(u_c - u)\left[\frac{1-w}{t_w^-}\right] - \Theta(u - u_c)\left[\frac{w}{t_w^+}\right]
\end{aligned} \tag{2}$$

DOI: 10.1002/fld

where $\Theta(x)$ denotes a Heaviside step function equal to 1 for $x \geqslant 0$ and 0 for $x < 0$. The currents in the equation above are described by

$$\begin{aligned} J_{\mathrm{fi}} &= -\frac{v}{t_d}\Theta(u-u_c)[(1-u)(u-u_c)] \\ J_{\mathrm{si}} &= -\frac{w}{2t_{\mathrm{si}}}[1+\tanh(k\{u-u_c^{\mathrm{si}}\})] \\ J_{\mathrm{so}} &= \frac{u}{t_0}\Theta(u_c-u)+\frac{1}{t_r}\Theta(u-u_c) \\ t_v^-(u) &= \Theta(u-u_v)t_{v1}^- + \Theta(u_v-u)t_{v2}^- \end{aligned} \tag{3}$$

where J_{fi} is the fast input current, J_{si} is the slow input current and J_{so} is the slow output current and the remaining parameters are described in the paper by Clayton and Holden [33].

The above model was solved numerically subject to zero flux conditions, for each of the three potentials, on the boundaries of the heart wall. The details of the solution procedure are summarized in Section 2.2, and the way in which the electric potential loads the structure is considered in Section 2.1.4.

2.1.2. The 'blood' fluid model. The 'blood' is modelled as a slightly compressible Newtonian fluid, which apparently reflects reality reasonably well [29, 30], where the density, ρ, is related to the pressure, p, by

$$\rho = v_1\left(1+\frac{p}{v_2}\right) \tag{4}$$

where the parameters v_1 and v_2 in Equation (4) are set equal to $10^3\,\mathrm{kg/m^3}$ and $10^6\,\mathrm{Pa}$, respectively. Hence, the flow should be well characterized by the Navier–Stokes (N–S) equations. Moreover the Reynolds numbers are such that the flow regime is reasonably well characterized as laminar. Thus, the fluid is modelled, as follows, for the ith component of momentum:

$$\frac{\partial(\rho u_i)}{\partial t}+\nabla\cdot(\rho\mathbf{u}u_i)=\nabla\cdot(\mu\nabla u_i)-\frac{\partial p}{\partial x_i}+S_i \tag{5}$$

where S_i contains all other terms in the equation such as sources and for a compressible fluid the extra diffusion terms. Mass conservation is expressed by

$$\frac{\partial\rho}{\partial t}+\nabla\cdot(\rho\mathbf{u})=S_m \tag{6}$$

where S_m includes any sources of mass.

The fluid is flowing within a domain that is itself moving, and this is catered in Section 2.1.4.

The locations of the boundary conditions for the flow, shown schematically in Figure 2, are as follows:

(a) A no slip wall condition on the interface between the blood and heart wall.
(b) While the heart wall is expanding the velocity at the inlet is set to the value required to provide sufficient blood to fill the increase in volume of the ventricle. During contraction the inlet is closed.

DOI: 10.1002/fld

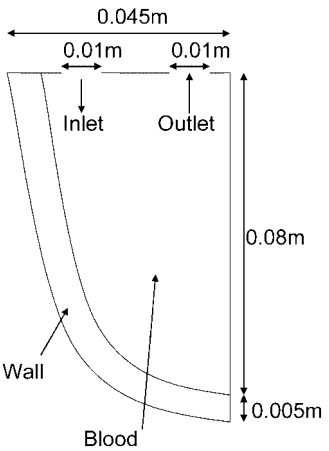

Figure 2. An illustration of the geometric cross section of the right ventricle of a human heart.

(c) A fixed pressure is specified at the outlet of the domain while the heart wall is contracting with the value calculated from the near outlet elements on the previous time step. The outlet is closed during expansion.

2.1.3. The structural mechanics model. This section sets out the governing and constitutive equations for structural mechanics of the ventricle, which is modelled as a simple elastic material. The universal law governing any continuum undergoing motion is given by Cauchy's equation:

$$\nabla \cdot \boldsymbol{\sigma} + \mathbf{b} = \rho \mathbf{a} \tag{7}$$

where $\boldsymbol{\sigma}$ is the stress tensor, $\mathbf{b}$ are body forces and $\mathbf{a}$ is the acceleration of the structure. In the system here, which is focussed on the coupling of the phenomena, the static form of this equation, $\mathbf{a} = \mathbf{0}$, is used. In reality the dynamic response of the ventricle wall will be an important component of a model of the heart. Details of how the structural dynamics would be resolved within the framework used here are presented in [22].

The generalized form of Hooke's law gives the following constitutive relationship between stress and strain for an isotropic homogeneous material undergoing small strains in three dimensions:

$$\boldsymbol{\sigma} = \mathbf{D}\boldsymbol{\varepsilon}_{\mathrm{el}} \tag{8}$$

where $\mathbf{D}$ is defined in terms of Young's modulus and Poisson's ratio in the conventional manner and $\boldsymbol{\sigma} = (\sigma_x, \sigma_y, \sigma_z, \sigma_{xy}, \sigma_{yz}, \sigma_{xz})^{\mathrm{T}}$ is the stress vector and $\boldsymbol{\varepsilon}_{\mathrm{el}} = (\varepsilon_x, \varepsilon_y, \varepsilon_z, \varepsilon_{xy}, \varepsilon_{yz}, \varepsilon_{xz})^{\mathrm{T}}$ is the elastic strain vector.

The initial approach to structural mechanics is based on a linear strain–displacement formulation using the small strain assumption, which is valid for strains of the order of a few percent [36]. Thus the strains may be decomposed into the product of the matrix of linear operators and the displacement vector which, for a three-dimensional approximation, enables the strains to be defined

DOI: 10.1002/fld

in the general displacement form:

$$\boldsymbol{\varepsilon} = \mathbf{L}\mathbf{d} \tag{9}$$

where $\mathbf{L}$ is the differential operator, $\boldsymbol{\varepsilon}$ is the total strain and $\mathbf{d}$ is the displacement vector [37]. Thus when only elastic strains are present, $\boldsymbol{\varepsilon}_{\mathrm{el}} = \boldsymbol{\varepsilon}$, Cauchy's equation may be expressed as

$$\mathbf{L}^{\mathrm{T}}(\mathbf{D}\mathbf{L}\mathbf{d}) + \mathbf{b} = \mathbf{0} \tag{10}$$

Equation (10) is subject on the surface $\Gamma = \Gamma_t \cup \Gamma_d$ to a traction and displacement boundary conditions, such that

$$\begin{aligned} \mathbf{R}^{\mathrm{T}}\boldsymbol{\sigma} &= \mathbf{t}_{\mathrm{p}} \quad \text{on } \Gamma_t \\ \text{and } \mathbf{d} &= \mathbf{d}_{\mathrm{p}} \quad \text{on } \Gamma_{\mathrm{d}} \end{aligned} \tag{11}$$

where $\mathbf{R}$ is the outward normal operator, $\mathbf{t}_{\mathrm{p}}$ are the prescribed tractions on the boundary Γ_t and $\mathbf{d}_{\mathrm{p}}$ are the prescribed displacements on the boundary Γ_{d}.

2.1.4. Coupling among the component phenomena. The couplings among the component models are conceived as follows and illustrated in Figure 3:

(a) The electric field, as represented by its potential, provides a load for the structure. The total strain now contains both an elastic and an electric component

$$\boldsymbol{\varepsilon} = \boldsymbol{\varepsilon}_{\mathrm{el}} + \boldsymbol{\varepsilon}_{\mathrm{elec}} \tag{12}$$

which results in an extra term in Equation (10). The electric strain is calculated from

$$\boldsymbol{\varepsilon}_{\mathrm{elec}} = -\alpha V(1, 1, 1, 0, 0, 0)^{\mathrm{T}} \tag{13}$$

where α is the electric strain equivalent of the thermal expansion coefficient in the thermal strain.

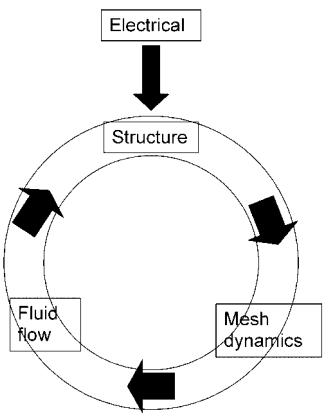

Figure 3. The overall solution strategy for the electro-fluid–structure coupling in a prototype computational model of the right ventricle of a heart.

DOI: 10.1002/fld

(b) The consequent interaction between the fluid and the structural domains is represented through a conventional fluid–structure interaction procedure:

- The traction load by the fluid on the structure is as follows [22, 23]:

$$\mathbf{t}_{\mathrm{p}} = (-p\mathbf{I} + \mu\{\nabla\mathbf{u} + (\nabla\mathbf{u})^{\mathrm{T}}\} - \tfrac{2}{3}\mu(\nabla\cdot\mathbf{u})\mathbf{I})\mathbf{n} \quad \text{on } \Gamma_s \tag{14}$$

  where p and μ are the fluid pressure and dynamic viscosity, respectively, $\mathbf{I}$ is the identity matrix and $\mathbf{n}$ is the normal to the fluid–structure interface.
- The deformation of the structure affects the fluid domain through a consistent movement of the fluid domain–structure boundary. In response to this boundary motion, the mesh in the fluid domain is adapted to maintain element quality. For moving domains it is essential that there is spatial conservation, that is, in the solution of the N–S equations above, a uniform flow is preserved for a moving domain. The geometric conservation law states that '*Change in volume of a domain within a time increment must equal the volume swept by the domain boundary during the time step*' [38], which is expressed by the following equation:

$$\frac{\partial V}{\partial t} - \int_V \nabla\cdot\mathbf{u}_{\mathrm{m}}\,\mathrm{d}V = 0 \tag{15}$$

  where V is the volume of the domain and $\mathbf{u}_{\mathrm{m}}$ is the boundary velocity. Thus the fluid velocity, $\mathbf{u}$, in the convection term of the N–S equation and the continuity equation must be replaced by the relative velocity $\mathbf{u}_{\mathrm{r}}$ which is given by

$$\mathbf{u}_{\mathrm{r}} = \mathbf{u} - \mathbf{u}_{\mathrm{m}} \tag{16}$$

  Details of the mesh adaption algorithm and the calculation of the mesh velocity can be found in [22].

2.1.5. Some critical comments on the model formulation. Although the above model is an attempt to emulate the main aspects of the heart function, it is not a viable model of the heart as it stands, for a range of reasons, which include:

(a) The blood flow is not Newtonian and is more properly represented by a non-Newtonian viscosity, such as Casson's law [39].
(b) The ventricle wall is neither simple elastic nor isotropic.
(c) A substantial debate still wages on the most appropriate way to embed the impact of the electric field within the structural calculation, and Smith *et al*. [9] provide a very useful survey of the current state of the art.
(d) The electro-chemical field is better described by more complex models such as that by ten Tusscher *et al*. [7].

However, it turns out that

(a) The broad flow characteristics of the flow within the ventricle are not very sensitive to the specific viscosity relationship used.

DOI: 10.1002/fld

(b) The structure of the ventricle wall is complex and to characterize it as a simple isotropic material provides the opportunity to capture the impact of contraction and relaxation in two dimensions reasonably well.
(c) Moreover since the predominant movement captured by this model is contraction–expansion, then the limitation of using a small strain model for a large strain behaviour is not abused too much.
(d) The simple electric strain formulation is justified on the basis that it is straightforward to implement and that there is no otherwise generally adopted model by the computational physiology community—when there is, this will be straightforward to adopt and implement here.
(e) The objective of this work is as a first step to a fully functional heart function model, and so in attempting to evaluate the broad cyclic behaviour reflected by the electrical–fluid–structure interactions, the Clayton–Holden electro-chemical model appears as adequate.

Finally, we should comment that we expect to address each of the above deficiencies as the project develops further and once we have established the viability of the basic heart function interactions.

2.2. The computational model

2.2.1. The numerical framework. The framework used is essentially one which features:

(a) an unstructured mesh in two and three dimensions, with a mix of elements from triangles and quadrilaterals in two dimensions and from tetrahedral to hexahedral elements in three dimensions—in this preliminary work we restrict the analysis to two dimensions;
(b) the discretization is focused on finite volume methods which in this application uses cell-centred approximations for the flow and the electric field calculations and vertex-based approximations for the structural mechanics.

Thus, a simplified model of the right ventricle from the heart wall of a human from [34] was constructed. Bearing in mind that the objective of this phase of the work was simply to test the viability of developing a model which would exhibit the broad function of a heart, then detailed validation was not an issue and so a mesh was selected that was consistent with the timescale of the most significant physical process—which turned out to be the electric field and enabled a conservative calculation that was reasonably accurate in time and space. Figure 2 shows the physical model with the dimensions and highlighting the inlet and outlet ports within the calculation.

2.2.2. The fluids solver. The fluids solver module uses a variant of the SIMPLE pressure correction solver [40] with a cell-centred discretization scheme which employs a Rhie–Chow interpolation scheme to counteract pressure checker-boarding. The velocity components and the pressure correction equations are solved using a diagonally pre-conditioned conjugate gradient solver. This procedure is described in some detail in Croft *et al*. [41], Croft [42], McBride [43] and McBride *et al*. [44], where it is evaluated on a number of benchmark problems.

2.2.3. The structural solver. In the structural solver, it is useful to consider the application of the method of weighted residuals to the equilibrium equation (10) subject to the boundary

DOI: 10.1002/fld

conditions, as expressed by equation (11), which then gives the familiar weak form of the equilibrium equations (17)

$$-\int_{\Omega}[\mathbf{LW}]^{\mathrm{T}}(\mathbf{DLd})\,\mathrm{d}\Omega+\int_{\Omega}[\mathbf{W}]^{\mathrm{T}}\mathbf{b}\,\mathrm{d}\Omega+\int_{\Gamma_{\mathrm{d}}}[\mathbf{RW}]^{\mathrm{T}}(\mathbf{DLd})\,\mathrm{d}\Gamma+\int_{\Gamma_t}[\mathbf{W}]^{\mathrm{T}}\mathbf{t}_{\mathrm{p}}\,\mathrm{d}\Gamma=\mathbf{0} \tag{17}$$

where $\mathbf{W}$ is a diagonal matrix of arbitrary weighting functions and $\mathbf{t}_{\mathrm{p}}$ is the fluid traction load on the target at the fluid target interface, which is given by equation (above). The unknown displacements, $\mathbf{d}$, may be approximated by

$$\mathbf{d}\approx\overline{\mathbf{d}}=\mathbf{N}_j\hat{\mathbf{d}}_j \quad (j=1,2,3,\ldots,n) \tag{18}$$

where $\mathbf{N}_j$ is a set of shape functions and $\hat{\mathbf{d}}_j$ is the displacement evaluated at the nodes. The displacement approximation (18) may be substituted into the equilibrium equation (17), where the arbitrary weighting functions $\mathbf{W}$ are replaced by a finite set of prescribed functions for each node. The equilibrium equation (17) may then be expressed as a linear system of equations of the form:

$$\mathbf{Kd}-\mathbf{f}=\mathbf{0} \tag{19}$$

where $\mathbf{K}$ is the global stiffness matrix, $\mathbf{d}$ is the global approximation to displacement and $\mathbf{f}$ is the global equivalent force vector. Further details of the spatial discretization of equation utilized here and its evaluation of on a range of benchmarks may be found in a number of references; see, for example, Bailey and Cross [45], Taylor *et al.* [46] and Slone *et al*. [47].

In the model of the ventricle all surfaces are regarded as free, except the top layer on each side of the solid structure, where in each case the displacement in the y-direction is fixed, as well as that in the x-direction at the inner most points of each layer. This ensures that although the solid structure responds to the pressure from the fluid and the impact of the electric field, it simply moves relative to this top layer.

2.2.4. The electric field solver. The group of equations in Section 2.1.1 were solved within the finite volume—unstructured mesh solver framework using the cell-centred discretization form. The resulting discretized equations were solved iteratively within the same iteration loop as the fluid flow. The following procedure was followed within each iteration:

(a) calculate the currents according to Equations (3);
(b) solve the u potential equation from (2) using an implicit discretization of the diffusion term;
(c) solve the v and w potential equations from (2) using the value of u calculated at the previous stage in the Heaviside functions.

A number of test problems were evaluated to ensure that the implementation here was comparable with that by Clayton and Holden [33]. They describe a test problem that is essentially a three-dimensional block of the following dimensions $82.5\,\mathrm{mm}\times 82.5\,\mathrm{mm}\times 16.5\,\mathrm{mm}$ subject to the no flux conditions at the boundary. Their explicit finite difference solver employed a mesh size of $0.33\,\mathrm{mm}^2$ and a time step of 0.1 ms. These numerical parameters produced a stable solution, i.e. modest changes in plane wave speed of less than 1% for time step increase of a factor of 2. Figure 4 shows results obtained using our model for the temporal variation of the three potentials and the

DOI: 10.1002/fld

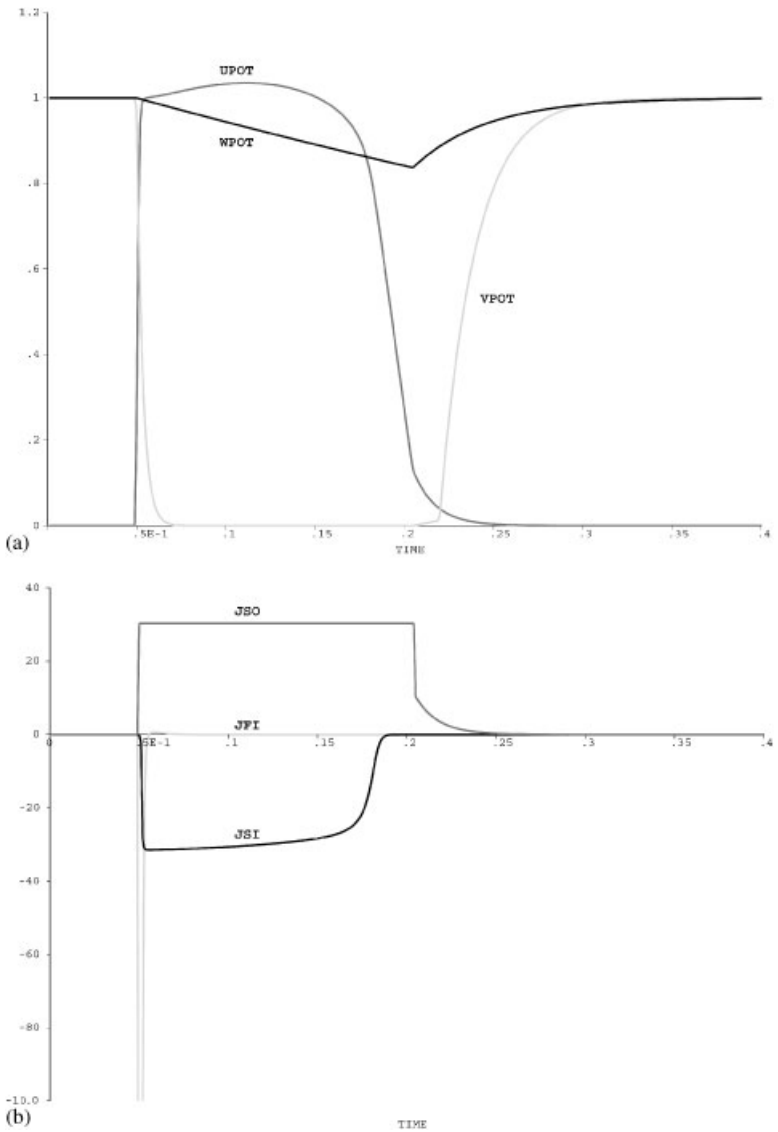

Figure 4. The computational predictions for the implementation of (a) the potentials and (b) the currents using the electro-chemical model of Clayton and Holden [33].

three currents. These results show excellent agreement with the results presented by Clayton and Holden in Figure 1 of [33].

2.2.5. The electrical–fluid–structure interaction solver strategy. Essentially the electric field provides at each time step, a measure of the electric strain, which is embedded within the structural calculation and provides a driving force to either contract or relax the ventricle wall.

DOI: 10.1002/fld

This structure then interacts with the fluid, which may be captured by a slightly simplified version of the dynamic fluid–structure interaction (DFSI) procedure of Slone *et al*. [22, 23]. The overall solution strategy is illustrated in Figure 3, and is summarized as follows:

At each new time step,

(a) Decide on flow boundary conditions as a function of the contraction—relaxation state of the ventricle wall.
(b) Apply the incremental update to the mesh.
(c) Update the mesh velocity.
(d) Iteratively solve the N–S equations for the net fluid velocity.
(e) Calculate and apply fluid load onto the structure.
(f) Calculate the electric strain load throughout the structure.
(g) Calculate the subsequent structural deformation.
(h) Calculate the consequent deformation of the flow domain mesh.

What is clear in the above procedure is that although the electric field is coupled into the fluid–structural calculation, it is essentially independent of it. In other words, the coupling of the electric field into the calculation is one way. Also, since we have made the electric strain directly proportional to the electric potential then as the potential field rises and falls then so does the strain. This means that we can calculate the electric field 'off-line' and use it to estimate when the ventricle is either pumping blood out from the system of drawing it in. These calculations were made and a time sequence for opening and closing the two valves at the top of the ventricle was devised—one acting as the inlet and the other as the outlet.

Hence, in summary the computational model is structured as follows: at each time step,

(a) The electric field is calculated by the Clayton and Holden model [33].
(b) The electric tensions are calculated and provided as a source into the structural calculation.
(c) The consequent fluid–structure procedure above is invoked.

Having said this, in fact, the procedure does not demand that each of the solvers has the same time step and indeed,

(a) The structural time step is 10^{-3} s.
(b) There are 10 fluid time steps to each structural time step.
(c) The electrical potentials are resolved using the same time step as the fluid.

The use of different time steps in the various models requires careful handling of the information transfer between the models. The traction load of the fluid on the solid is mainly a pressure load. Each mesh face on the interface between the fluid and structure calculates its own time-averaged pressure over the time between structural analyses. This is then used to calculate the pressure load applied to the solid. The electric strain is calculated from the voltage. For this quantity the voltage at the time of the structural analysis is used. Feeding the structural deformation back into the fluid model in particular and the electrical model has to be handled carefully. An instantaneous update of the mesh in line with the predictions of the structural analysis results in a significant pressure shock that the fluid often fails to handle. Consequently the mesh is moved incrementally over the fluid time steps between structural analyses. This full deformation of the fluid–solid interface is only applied on the time step preceding the next structural analysis.

DOI: 10.1002/fld

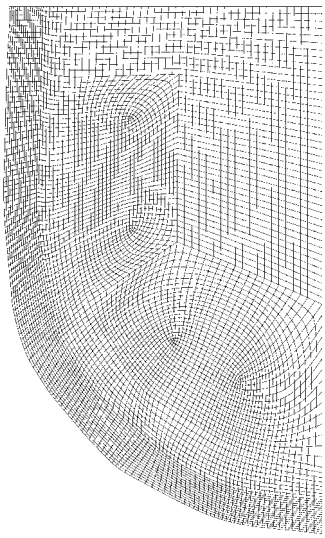

Figure 5. The mesh used in the analysis of the electro-fluid–structural ventricular system.

2.2.6. Calculation details for the ventricle model. The mesh of 6602 quadrilateral elements is shown in Figure 5. The parameters for the electrical calculation are all as shown in Clayton and Holden [33]. The fluid properties are assumed to be close to those of water (density $= 1000\,\mathrm{kg/m^3}$ at atmospheric pressure; viscosity $= 3 \times 10^{-3}\,\mathrm{Pa/s}$). The structural wall is assigned the following properties (density $= 1000\,\mathrm{kg/m^3}$; Young's modulus $= 4 \times 10^8\,\mathrm{Nm}$; and Poisson's ratio $= 0.37$).

At the initiation of the simulation the flow field is assumed static, the strain is set to zero. The three potential variables, u, v and w from Equation (2), are initialized to 0, 1 and 1, respectively, with the electro-chemical pulse initiated by set the u potential to 0.2 over a selected area of the heart wall.

The time step for the structural calculation is as shown above, and for the fluid and electrical calculations it is set by the ratios above. The total time for the simulation is 0.3 s so involving 3000 fluid time steps. The calculations were performed on a DELL INTEL 3 GHz Pentium 4 processor with 1 GB core memory running under Windows and using an Intel Fortran compiler. The computation time for a simulation was about 12 h. The computational model was implemented within the open multi-physics software environment, PHYSICA [48].

3. COMPUTATIONAL MODEL RESULTS

Figure 6 shows some snap shots of the heart as it simultaneously

- Experiences the development and collapse of the electric potential field.
- The contraction and recovery of the heart wall.
- The blood effectively being pumped out from and then sucked into the heart-like vessel.

In the early stages we see the electric potential developing—building and spreading throughout the ventricular wall. Eventually, as the development peaks we see a drop in potential; it collapses

DOI: 10.1002/fld

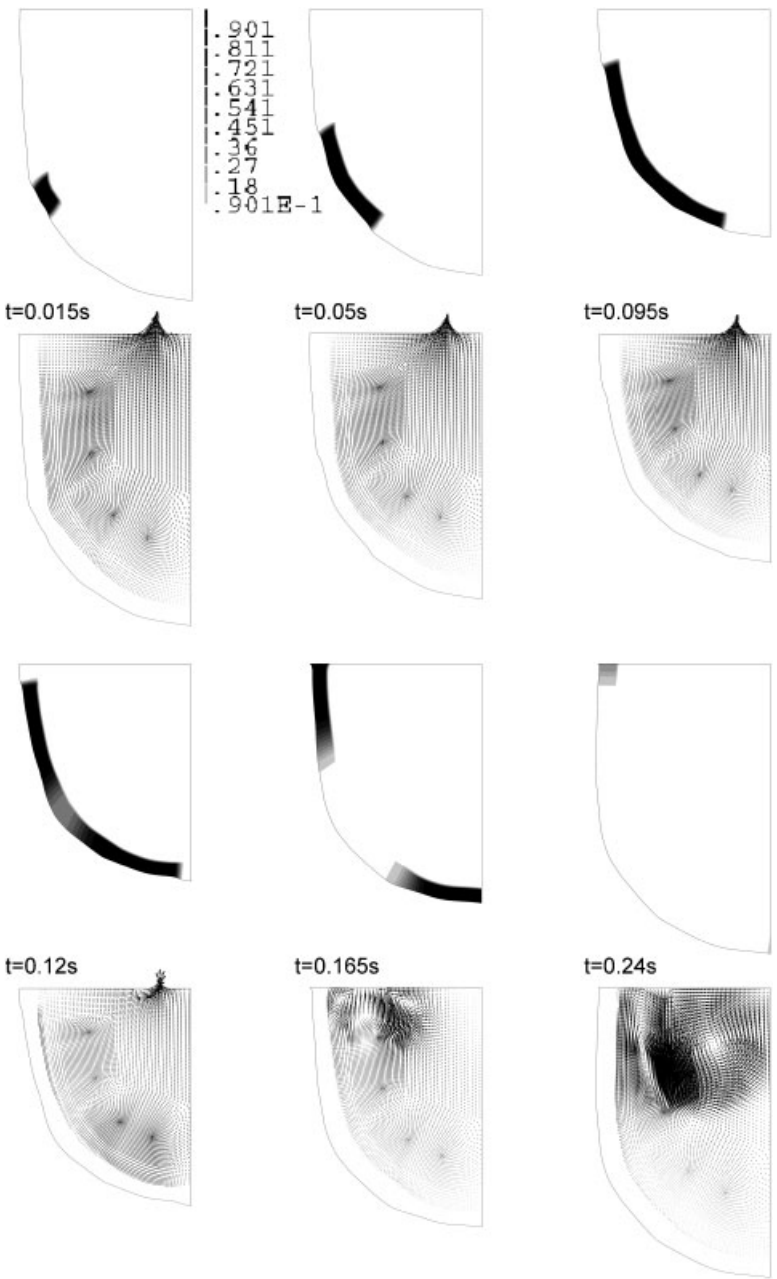

Figure 6. The development of the electric potential field (left) and the fluid flow field (right) over the 'heart-like' beat cycle.

DOI: 10.1002/fld

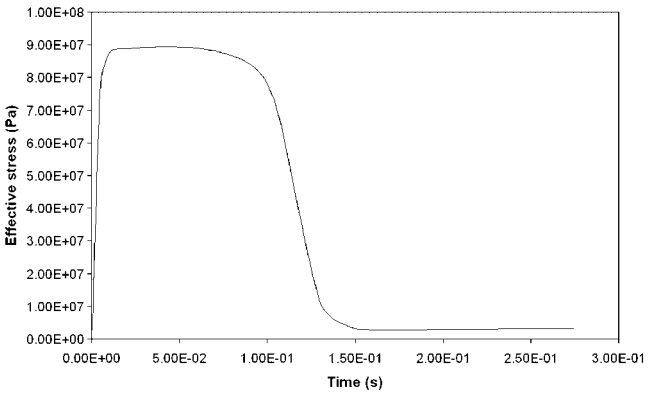

Figure 7. The development of stress within the ventricular wall throughout the systolic cycle.

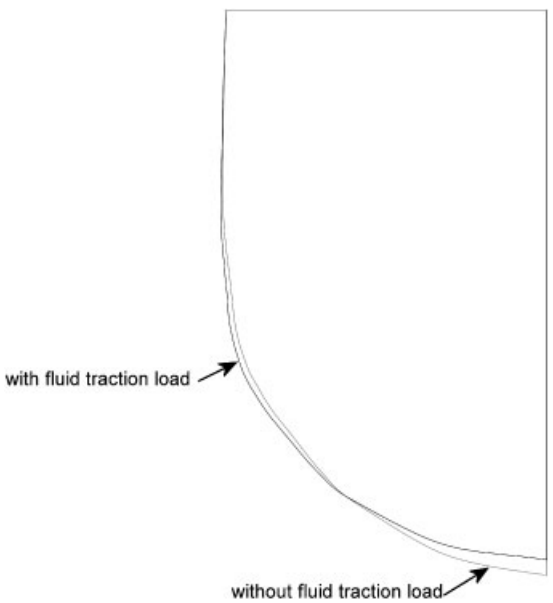

Figure 8. A comparison of the deformation of the ventricular domain with and without the traction load from the fluid.

at its centre back to its initial value (of zero), and the potential waves then progress outwards to the edge of the structural domain, followed by the propagation of the collapse until the whole structural domain is back to its initial condition. The consequence of the electric potential change is that in the early developing phase, the growing potential is introducing tension into the wall and causes it to contract. The contraction itself causes the fluid to flow out of the domain through the outlet boundary. The contraction itself combined with the flow out of the boundary then induces a gross circulatory flow with a number of secondary vortices. As the potential collapses, the wall begins to relax, so the outlet closes and the inlet opens. When this happens fluid is sucked into the

DOI: 10.1002/fld

domain and a new circulatory flow pattern is quickly established. Figure 7 shows the variation of stress development and subsequent complete relaxation at the centre of the ventricular wall during the systolic cycle.

One question that is worth asking in this context is the extent to which the fluid traction on the wall surface influences the change in geometry during the systolic cycle. Figure 8 shows the difference between the deformation with and without the inclusion of the traction force. As is plain the impact of the traction force on the geometrical shape of the ventricle is marginal.

These are very preliminary results, but provide an indication of the capability of a carefully conceived computational procedure for capturing the key complex interactions of an important closely coupled multi-physics system, such as, the heart.

4. CONCLUSIONS

A sufficiently comprehensive computational model has many potential applications in the evaluation of surgical procedures, assessing the operation of circulatory support devices and the response of the heart to novel drug regimes. Sophisticated mathematical models of each aspect of the heart function are now emerging. However, a comprehensive computational model of the whole heart function must be based on the computational representation of the electro-chemical function together with the interaction between the fluid and structural components. To implement such a computational model, it is vital to capture of the electro-chemical-fluid–structure interactions in a numerically robust fashion.

Hence, the objective of this work is to develop a solution procedure for capturing the nature of the interaction among the electrical, structural and flow fields in the context of a single ventricle as a model framework. In just about every aspect simplified component models have been used; however, the attempt has been made to include sufficient physical reality to enable the interactions to be defined and then captured in a numerically sound fashion.

Hence, the mathematical model couples together two well mathematical models and computational procedures:

(a) the Clayton–Holden model [33] of the electrical potential field as a simplified electro-chemical formulation.
(b) the fully DFSI developed by Slone *et al*. [22, 23].

A very preliminary mathematical model of the ventricular behaviour of the heart was defined by

(a) representing blood flow as a Newtonian fluid with the properties of water;
(b) capturing the structure of the ventricular wall as a simple elastic isotropic material;
(c) assuming the structure deforms to equilibrium at each time step.

The coupling between the two procedures of Clayton–Holden and Slone was affected by a definition of a simple relationship capturing the impact of the electrical field on the structure by a simple linear electrical strain based on its primary potential. The computational procedure was then assembled and tested on a two-dimensional cross section of the right ventricle of a human heart geometry.

Given the exploratory nature of this work it was neither possible nor appropriate to try and deliver a fully validated model, but the results were considered as reasonably mesh independent. However, the numerical procedure was quite stable and demonstrated a capability to reflect the electrically

DOI: 10.1002/fld

induced pumping behaviour of a heart-like structure, capturing the impact of the contraction and relaxation of the heart wall as a function of the electric field, and its subsequent action on the enclosed fluid domain together with its pumping out and sucking phases.

Now that a robust procedure has been constructed to capture the electrical–fluid–structural field interactions, the next phase of the project will involve

(a) a full three-dimensional geometrical model;
(b) a more comprehensive electro-chemical model based on the work of ten Tusscher *et al.* [7];
(c) a more realistic representation of blood as a non-Newtonian slightly compressible fluid;
(d) a much more realistic representation of the material structure of the wall [9];
(e) resolution of the dynamic response of the ventricle wall.

REFERENCES

1. Noble D. Modeling the heart—from genes to cells to the whole organ. *Science* 2001; **295**:1678–1682.
2. Hodgkin AL, Huxley AF. A quantitative description of membrane current and its application to conduction and excitation in nerve. *Journal of Physiology* 1952; **117**:500–544.
3. Noble D. Cardiac action and pacemaker potentials based on the Hodgkin–Huxley equations. *Nature* 1960; **188**:495–497.
4. Trayanova N, Li W, Eason J, Kohl P. Effect of stretch-activated channels on defibrillation efficacy. *Heart Rhythm* 2004; **1**:67–77.
5. Plank G, Vigmond EJ, Leon LJ. The shock energy required for successful defibrillation depends on the degree of disorganisation of the re-entrant activation pattern. *Cardiovascular Engineering* 2004; **4**:149–154.
6. Sundnes J. Numerical methods for simulating the electrical activity of the heart. *Ph.D. Thesis*, University of Oslo, Norway, 2002.
7. ten Tusscher KHWJ, Noble D, Noble PJ, Panilov AV. A model for human ventricular tissue. *American Journal of Physiology—Heart and Circulatory Physiology* 2004; **286**:1573–1589.
8. Nickerson DP, Smith NP, Hunter PJ. A model of cardiac cellular electromechanics. *Philosophical Transactions of the Royal Statistical Society of London Series A* 2001; **359**:1159–1172.
9. Smith NP, Nickerson DP, Crampin EJ, Hunter PJ. Multi-scale computation modelling of the heart. *Acta Numerica* 2004; **13**:371–431.
10. Nash MP, Hunter PJ. Computational mechanics of the heart: from tissue structure to ventricular function. *Journal of Elasticity* 2000; **61**:113–141.
11. LeGrice I, Hunter P, Young A, Smaill B. The architecture of the heart: a database model. *Philosophical Transactions*: *Mathematical*, *Physical and Engineering Sciences* 2001; **359**:1217–1232.
12. Costa KD, Holmes JW, McCulloch AD. Modelling cardiac mechanical properties in three dimensions. *Philosophical Transactions of the Royal Statistical Society of London Series A* 2001; **359**:1233–1250.
13. Markhasin VS, Solovyova O, Katsnelsona LB, Protsenkoa Y. Mechano-electric interactions in heterogeneous myocardium: development of fundamental experimental and theoretical models. *Progress in Biophysics and Molecular Biology* 2003; **82**:207–220.
14. Nash MP, Panifilov AV. Electromechanical model of excitable tissue to study re-entrant cardiac arrhythmias. *Progress Biophysics and Molecular Biology* 2004; **85**:501–522.
15. Smith NP. A computational study of the interaction between coronary blood flow and myocardial mechanics. *Physiological Measurement* 2004; **25**:863–877.
16. Haslach HW. Nonlinear viscoelastic thermodynamically consistent models for biological soft tissue. *Biomechanics and Modeling in Mechanobiology* 2005; **3**:172–189.
17. Usyk TP, LeGrice IJ, McCulloch AD. Computational model of three dimensional cardiac electromechanics. *Computing and Visualization in Science* 2002; **4**:249–257.
18. Arts T, Bovendeerd, Delhaas T, Prinzen F. Modeling the relation between cardiac pump function and myofiber mechanics. *Journal of Biomechanics* 2003; **36**:731–736.
19. Farhat C, Lesoinne M, Maman M. Mixed explicit/implicit time integration of coupled aeroelastic problems: three field formulation geometric conservation and distributed solution. *International Journal for Numerical Methods in Fluids* 1995; **21**:807–835.

DOI: 10.1002/fld

20. Mok DP, Wall W. Partitioned analysis schemes for the transient interaction of incompressible flows and nonlinear flexible structures. *Trends in Computational Structural Mechanics*. CIMNE: Barcelona, Spain, 2001; 689–698.
21. Mattheis HG, Steindorf J. Partitioned strong coupling algorithms for fluid–structure interaction. *Computers and Structures* 2003; **81**:805–812.
22. Slone AK, Pericleous K, Bailey C, Cross M. Dynamic fluid–structure interaction using finite volume unstructured mesh procedures. *Computers and Structures* 2002; **80**:371–390.
23. Slone AK, Pericleous K, Bailey C, Cross M, Bennett C. A finite volume unstructured mesh approach to dynamic fluid–structure interaction: an assessment of the challenge of predicting the onset of flutter. *Applied Mathematical Modelling* 2004; **28**:211–239.
24. Peskin CS, McQueen DM. Modeling prosthetic heart valves for numerical analysis of blood flow in the heart. *Journal of Computational Physics* 1980; **37**:113–132.
25. Peskin CS, McQueen DM. A three dimensional computational model of blood flow in the heart I. Immersed elastic fibers in a viscous incompressible fluid. *Journal of Comparative Physiology* 1989; **81**:372–405.
26. McQueen DM, Peskin CS. A three dimensional computational model of blood flow in the heart II contractile fibers. *Journal of Comparative Physiology* 1989; **82**:289–297.
27. Kovacs SJ, McQueen DM, Peskin CS, Modelling cardiac fluid dynamics and diastolic function. *Philosophical Transactions of the Royal Statistical Society of London Series A* 2001; **359**:1299–1314.
28. de Hart J, Baajens FPT, Peters GWM, Schreurs PJG. A computational fluid–structure interaction analysis of a reinforced stentless aortic valve. *Journal of Biomechanics* 2003; **36**:699–712.
29. Patterson EA, Carmody CJ, Howard I. Simulating the motion of heart valves under fluid flows induced by cardiac contractions. *Proceedings of the 6th International LS-DYNA Users Conference*, Dearborn, Michigan, U.S.A., 2000; 13.15–13.20.
30. Carmody C, Burriesci G, Howard I, Patterson EA. The use of LS-DYNA fluid–structure interaction to simulate fluid driven deformation in the aortic valve. *Proceedings of the 4th European LS-DYNA Users Conference*, Ulm, 2003; 1-1-11–1-1-20.
31. Watanabe W, Segiura S, Kafuku H, Hisada T. Multiphysics simulation of the left ventricular filling dynamics using fluid–structure interaction finite element method. *Biophysical Journal* 2004; **87**:2074–2085.
32. Luo C, Rudy Y. A model of the ventricular cardiac action potential depolarisation, repolarisation and their interaction. *Circulation Research* 1991; **68**:1501–1526.
33. Clayton RH, Holden AV. A method to quantify the dynamics and complexity of re-entry in computational models of ventricular fibrillation. *Physics in Medicine and Biology* 2002; **47**:225–238.
34. Grays Anatomy. http://www.bartleby.com/107/133.html (Accessed 11 July 2007).
35. Fenton F, Karma A. Vortex dynamics in three dimensional continuous myocardium with fiber rotations: filament instability and fibrillation. *Chaos* 1998; **8**:20–47.
36. Fenner RT. *Engineering Elasticity*: *Applications of Numerical and Analytical Techniques*. Ellis Horwood: Chichester, U.K., 1986.
37. Onate E, Cervera M, Zienkiewicz OC. A finite volume format for structural mechanics. *International Journal for Numerical Methods in Engineering* 1994; **37**:181–201.
38. Lesoinne M, Farhat C. Geometric conservation laws for flow problems with moving boundaries and deformable meshes and their impact upon aeroelastic equations. *Computer Methods in Applied Mechanics and Engineering* 1996; **134**:71–90.
39. Oka S. Pressure development in a non-Newtonian flow through a tapered tube. *Rheologica Acta* 1973; **12**(2):224–227.
40. Patankar SV, Spalding DB. A calculation procedure for heat, mass and momentum transfer in three dimensional parabolic flows. *International Journal of Heat and Mass Transfer* 1972; **15**:1787–1806.
41. Croft TN, Pericleous KA, Cross M. PHYSICA: a multi-physics environment for complex flow processes. In *Numerical Methods for Laminar and Turbulent Flow '95*, Taylor C, Durbetaki P (eds). Pineridge: Swansea, 1995; 1269–1280.
42. Croft TN. Unstructured mesh finite volume algorithms for swirling turbulent reacting flows. *Ph.D. Thesis*, University of Greenwich, London, 1998.
43. McBride D. Vertex based discretisation methods for thermo-fluid flow in a finite volume unstructured mesh context. *Ph.D. Thesis*, University of Greenwich, London, 2003.
44. McBride D, Croft TN, Cross M. Finite volume method for the solution of flow on distorted meshes. *International Journal of Numerical Methods for Heat and Fluid Flow* 2007; **17**:213–239.
45. Bailey C, Cross M. A finite volume procedure to solve elastic solid mechanics problems in three dimensions on an unstructured mesh. *International Journal of Numerical Methods in Engineering* 1995; **38**:1757–1776.

DOI: 10.1002/fld

46. Taylor GA, Bailey C, Cross M. A vertex based finite volume method applied to non-linear material problems in computational solid mechanics. *International Journal of Numerical Methods in Engineering* 2003; **56**:507–529.
47. Slone AK, Bailey C, Cross M. Dynamic solid mechanics using FV methods. *Applied Mathematical Modelling* 2003; **27**:69–87.
48. PHYSICA. see http://www.physica.co.uk (Accessed 11 July 2007).

DOI: 10.1002/fld